Separation Science and Technology
Publication details, including instructions for authors and subscription information:
http://www.informaworld.com/smpp/title~content=t713708471

Purification of L-Phenylalanine from a Ternary Amino Acid Mixture Using a Two-Zone SMB/Chromatography Hybrid System

Jin Seok Hur[a]; Phillip C. Wankat[a]; Jin-Il Kim[b]; Jeung Kun Kim[b]; Yoon-Mo Koo[b]
[a] School of Chemical Engineering, Purdue University, West Lafayette, Indiana, USA [b] Department of Biological Engineering, ERC for Advanced Bioseparation Technology, Inha University, Incheon, Korea

To cite this Article Hur, Jin Seok , Wankat, Phillip C. , Kim, Jin-Il , Kim, Jeung Kun and Koo, Yoon-Mo(2007) 'Purification of L-Phenylalanine from a Ternary Amino Acid Mixture Using a Two-Zone SMB/Chromatography Hybrid System', Separation Science and Technology, 42: 5, 911 — 930
To link to this Article: DOI: 10.1080/01496390701206264
URL: http://dx.doi.org/10.1080/01496390701206264

Separation Science and Technology, 42: 911–930, 2007

ISSN 0149-6395 print/1520-5754 online
DOI: 10.1080/01496390701206264

Purification of L-Phenylalanine from a Ternary Amino Acid Mixture Using a Two-Zone SMB/Chromatography Hybrid System

Jin Seok Hur and Phillip C. Wankat
School of Chemical Engineering, Purdue University, West Lafayette, Indiana, USA

Jin-Il Kim, Jeung Kun Kim, and Yoon-Mo Koo
Department of Biological Engineering ERC for Advanced Bioseparation Technology, Inha University, Incheon, Korea

Abstract: A two-zone SMB/chromatography hybrid system was studied to separate L-phenylalanine, which is the intermediate retained component, from a ternary amino acid mixture; glycine, L-phenylalanine, and L-tryptophane. PVP (poly-4-vinylpyridine) and deionized water were used as solid and liquid phases, respectively. Single component linear isotherms and mass transfer rates were obtained from multiple frontal tests. For the mass transfer rate, the Lapidus and Amundson linear dispersion model was used with an effective dispersion coefficient calculated from the mass transfer rate and the axial dispersion coefficient. This model was validated by comparing the frontal data with the simulation results from Aspen Chromatography 2004®. A single objective genetic algorithm was employed to determine optimal operating condition. Experiments using the two-zone SMB/chromatography system were conducted to purify L-phenylalanine. The results show that the two-zone system successfully removed 95.0% of glycine and 79.2% of L-tryptophane from the ternary mixture producing a L-phenylalanine product purity of 88.2%.

Keywords: Adsorption, amino acids, chromatography, simulated moving bed

Received 23 May 2006, Accepted 29 November 2006
Address correspondence to Prof. P. C. Wankat, School of Chemical Engineering, Purdue University, 480 Stadium Mall Drive, West Lafayette, IN 47907-2100, USA. Tel.: 765-494-7422; E-mail: wankat@ecn.purdue.edu

INTRODUCTION

In recent studies, four-zone simulated moving bed (SMB) systems have shown higher throughput, recovery, and purity compared to conventional chromatography processes (1–4). Because of these advantages, the SMB process has become an attractive alternate to chromatographic separations, especially for binary mixtures. In addition, many techniques have been proposed to increase the efficiency of SMB systems (5–11) including the VARICOL process (7, 8), partial (or power) feed (9, 10), and selective withdrawal (11).

In general, more than two components are involved in industrial separations. For complete multicomponent separations, the obvious approach is to use multiple binary four-zone SMBs. For example, two coupled SMBs may be used for complete ternary separations (12–15). In the first SMB unit, ternary feed is separated into a binary mixture and a product, and then the second SMB separates the binary mixture into two products. Although the design is robust, it requires many columns and often an additional separation unit to remove excess mobile phase between trains. There also have been studies in single train systems with fewer zones. Masuda et al. patented a single four-zone SMB process using a discontinuous feed stream for ternary mixtures (16), and a five-zone SMB has been extensively studied (17–23). However, the single train systems can produce pure products only when the intermediate and most retained components are easy to separate.

Multicomponent separations often require the purification of only one component. Examples include xylene separation (24, 25), insulin purification (26, 27), sugar separation (28, 29), and chiral separation (7, 30). The binary four-zone SMB can be employed to separate the most or least retained component from a multicomponent mixture by considering the mixture as pseudo-binary (24, 30). However, if one of the intermediate retained components is the only desired product, which we call a "*center-cut separation*," a series of multiple binary SMBs is often used (15, 26–28). Figure 1 shows a general cascade with two four-zone SMBs for ternary mixtures. In the figure, A, B, and C are the least, intermediate, and most retained components, respectively. This design is robust but complex and expensive.

For a single cascade process for the center-cut separation, we previously (31) developed a two-zone SMB/chromatography hybrid system (Fig. 2). Similar systems have been developed for complete ternary separations when the B-C separation is easy (32), and for separation of a quaternary mixture system (33). In the two-zone system, A and B are separated by a SMB approach (the switching and remixing with the feed keep the mass transfer zone inside the column) while the B-C separation is chromatographic (the B-C mass transfer zone leaves the system). During step *a*, the slowest component C from the previous feed step exits with the fast moving component A at the top of zone 1, and AB is recycled from zone 2 by remixing with feed. During step *b*, AC and B products are produced at the exits of zones 1 and 2, respectively. Although a relatively large selectivity between the intermediate and most retained components is

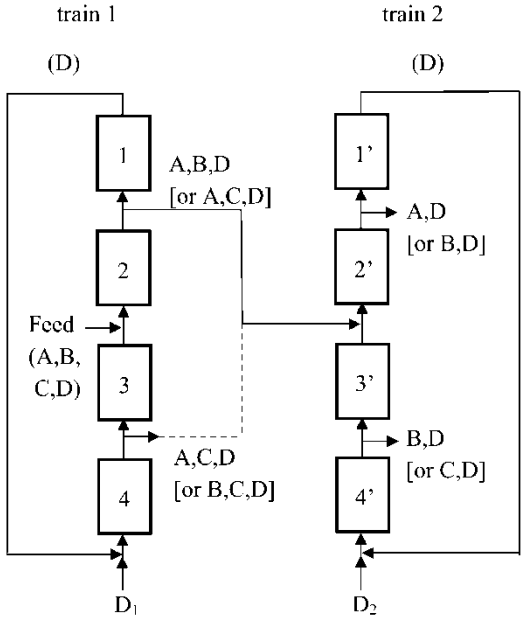

Figure 1. Cascade with two four-zone SMBs to separate only the intermediate component B from a ternary mixture. Switching of ports is not shown.

required, the previous studies using Aspen simulations showed that the two-zone system effectively works with fewer columns compared to a cascade with multiple four-zone SMBs (31, 33).

The goal of this study is to experimentally prove the concept of the two-zone SMB/chromatography hybrid process. For the experimental study, the ternary mixture of amino acids; glycine (A), L-phenylalanine (B), and L-tryptophane (C) was chosen as a model system. To estimate single component isotherms and mass transfer parameters, multiple frontal tests were conducted, and the concentration profiles from the frontal analysis were compared with Aspen simulation results produced with the estimated parameters. A binary coded genetic algorithm was used to determine optimum operating conditions, and then SMB experiments using the two-zone system were conducted.

THEORY AND SIMULATION MODEL FOR SMB

Local Equilibrium Design

The local equilibrium model has been widely used to analyze SMB systems since it is simple to use and helps visualize solute movements in columns.

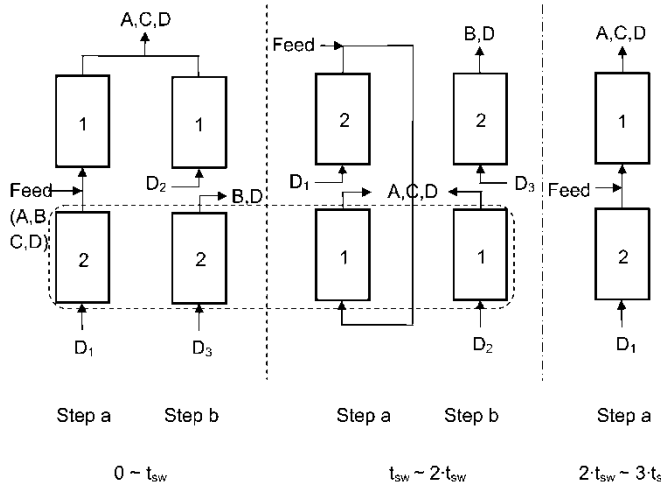

Figure 2. Integrated two-zone SMB/chromatography system for center-cut separation from a ternary mixture (24). Reprinted with permission from *Ind. Eng. Chem. Res.*, Copy right 2006.

Although various versions of the local equilibrium model have been proposed and used (14, 20, 31–35), the model is particularly simple when the isotherms are linear. Since the experimental isotherms were linear, the solute velocity for a single porosity model is (36),

$$u_{ijk} = \frac{v_{jk}}{1 + [1 - \varepsilon/\varepsilon]K_i} = G_i v_{jk} \tag{1}$$

where u_{ij} is the velocity of solute i in column j, v_{jk} is the superficial velocity in column j for step k, K_i is the linear equilibrium constant ($q_i = K_i C_i$), and G_i is the constant to determine the velocity of solute. For the center-cut separation with the two-zone SMB/chromatography system, the separation constraints based on the local equilibrium model were reported previously (31).

Instead of the selectivity, $\alpha_{j,i} = K_j/K_i$, the difficulty of separation was classified by $\alpha'_{i,j}$ defined as (14),

$$\alpha'_{i,j} = \frac{u_i}{u_j} = \frac{G_i}{G_j} \geq 1.0 \tag{2}$$

The $\alpha'_{i,j}$ is a better measure of difficulty for small K_i.

Linear Dispersion Model

In order to describe non-ideal concentration changes in a chromatography column, axial dispersion and mass transfer resistance should be considered.

We used the simple single porosity model,

$$\varepsilon \frac{\partial C_i}{\partial t} + (1-\varepsilon)\frac{\partial q_i}{\partial t} + \varepsilon \frac{\partial (vC_i)}{\partial z} - D_{ax,i}\frac{\partial^2 C_i}{\partial z^2} = 0 \tag{3}$$

The subscript i indicates the different solutes, C and q are the solute concentrations in liquid and solid phases, ε is the total porosity, and D_{ax} is the axial dispersion coefficient. The Chung and Wen correlation was used to estimate D_{ax} (37).

$$Pe_{d_p} = \frac{0.2}{\varepsilon} + \frac{0.011}{\varepsilon} Re^{0.48} \quad (10^{-3} < \mathrm{Re} < 10^3) \tag{4}$$

For mass transfer between solid and liquid phases, linear driving force was assumed and the lumped mass transfer model was used.

$$\frac{\partial q_i}{\partial t} = k_{eff,i} a_p (C_i^* - C_i) \tag{5}$$

where $k_{eff,i}$ is the mass transfer coefficient of component i, $a_p = 6/d_p$ for spherical particles and C^* is the solute concentration in the liquid phase at equilibrium. The mass transfer coefficients were estimated from the experimental data.

The Lapidus and Amundson linear dispersion model for a sufficiently long column with an apparent axial dispersion coefficient D_{ap} is (38),

$$C_i = \frac{C_{feed,i}}{2}\left[1 - erf\left(\frac{z - (vt/1 + (1-\varepsilon/\varepsilon)K_i)}{\sqrt{(4D_{ap,i}t/1 + (1-\varepsilon/\varepsilon)K_i)}}\right)\right] \tag{6}$$

When isotherms and porosity are known, D_{ap} can be obtained from frontal analysis data by nonlinear regression. In linear systems, zone spreading presented by D_{ap} depends on axial dispersion D_{ax} and the effective mass transfer coefficient k_{eff}. Dunnebier et al. determined the relation of these three parameters (39).

$$D_{ap,i} = D_{ax} + \frac{v^2 K_i}{k_{eff,i} a_p} \frac{k_i}{(1+k_i)^2} \tag{7}$$

where the capacity factor k_i is,

$$k_i = \frac{1-\varepsilon}{\varepsilon} K_i \tag{8}$$

The profiles determined with this model agree well with detailed simulations (9). Since the apparent dispersion coefficient D_{ap} can be estimated by using equation (6) to fit the data and the axial dispersion coefficient D_{ax} can be estimated with Equation (4), the lumped mass transfer coefficient k_{eff} is the only remaining unknown after isotherms and porosity have been determined. Equation (7) can then be used to determine k_{eff}.

The operation of the two-zone system is represented by D_{total}/F, purity P_B, and recovery R_B. D_{total}/F is the ratio of the total amount of desorbent to the amount of feed during a switching time. Other variables are defined as

$$P_B(\%) = \left[\frac{C_B}{C_A + C_B + C_C}\right]\text{in B product stream} \times 100 \tag{9}$$

$$R_B(\%) = \frac{[C_B \times Q_B]\text{ in B product stream}}{[C_B \times Q_{feed}]\text{ in feed stream}} \times 100 \tag{10}$$

The numerical solution of the algebraic and differential equations for packed beds was obtained by a biased upwind differencing scheme (BUDS) using Aspen Chromatography 2004® (40). In the simulations, 60 nodes per column were used, and the integration step was $t_{sw}/2000$. Numerical studies showed that these conditions were sufficient to obtain good numerical accuracy. A Pentium 2.4GHz PC with 512 MB RAM was used for simulations and approximately 10 minutes (clock time) were required to reach cyclic steady state.

EXPERIMENT

Materials

To measure the column porosity, NaCl was purchased from Sigma Chemical Co. (St. Louis, MO, US). The three amino acids; glycine (A), L-phenylalanine (B), and L-tryptophane (C) were also purchased from Sigma Chemical Co. (St. Louis, MO, US), and they have 98% minimum purity. The adsorbent PVP (poly-4-vinylpyridine cross-linked, Reillex HP polymer) was purchased from Reilly Industries Inc. (Indianapolis, IN, US), and pretreated with 1M NaOH, 1M HCl, and then 50% NaOH. After each step in the pretreatment, the resin was washed with deionized water (DIW), which was also used as the mobile phase. It was produced from Mili-Q system (Bedford, MA, US), and filtered with 0.22 μm filters. The mobile phase and solutions were degassed prior to experiments by sonicating in an ultrasonic bath with a vacuum pump.

Equipment

The glass columns (30 × 1.1 cm ID) were purchased from Ace Glass Co. (Vineland, NJ, US), and used for both frontal tests and SMB experiments. A fast protein liquid chromatography (FPLC, Amersham Bioscience, Piscataway, NJ, US) was used for frontal tests. A conductivity detector was used for NaCl pulse tests, and a UV detector with the wavelength of 254 nm was used to measure L-phenylalanine and L-tryptophane. Since glycine did not show clear resolution with the UV detector, a RI detector (Younglin

RI750F) was used for glycine. Two pumps in the FPLC controlled the flow of solution and mobile phase. For concentration measurement of product samples from the SMB experiments, an HPLC (LC-10AD, Shimadzu) with a column (15 × 0.46 cm ID), pump (LC-6AD), RI (RID-10A) and PDA (SPD-M10A) detectors was used.

A lab scale two-zone SMB/chromatography system is shown in Fig. 3. Figures 3a and 3b present flow and pump configurations for step a and b, respectively. The system consists of the two glass columns, four rotary valves (VICI, Switzerland), two FPLC pumps (Amersham Bioscience, Piscataway, NJ, US), and two HPLC pumps (Younglin Biochrom, Busan, Korea). The four pumps controlled flow rates of the feed and the three desorbent streams. The 16 position valves were controlled with Lab View (National Instruments, TX, US). The dead volume without the columns was 2.30 ml. The dead volume inside the columns was assumed to be negligible.

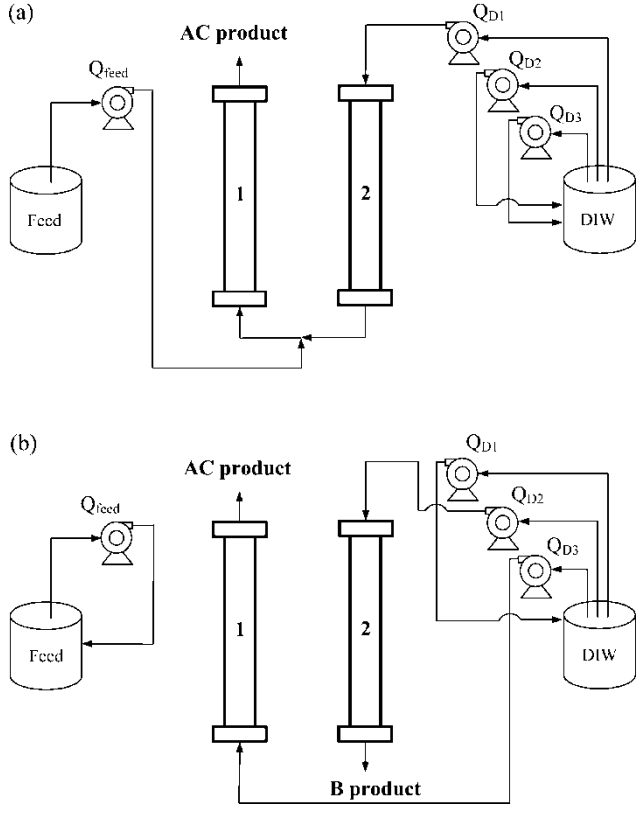

Figure 3. Two-zone SMB/chromatography equipment and configurations for experiment. a. step a b. step b.

Table 1. Column porosities from NaCl pulse tests

Column	Retention time (min)	u (cm/min)	v (cm/min)	ε
1	19.750	1.519	1.052	0.693
2	20.020	1.499	1.052	0.702
Average	19.885	1.509	1.052	0.698

Measurements

The columns were packed with the PVP by the slurry method using the FPLC at a flow rate of 10 ml/min for over 10 hours. Total porosity was measured from the retention time of the NaCl pulse test. Table 1 shows retention times, that were adjusted with the dead volume of tubes (0.74 ml), and porosities for each column. The difference in the two column porosities is only 1.3%. Thus, we averaged them for the total porosity, which was 0.698, rounded off to 0.70.

For isotherm measurements, frontal analysis was conducted with FPLC at 50°C. The flow rate was 1 ml/min, and the fraction of the amino acid in the inlet stream was increased by 20% for each step. Time for the step was determined from pulse tests with the single component and the mixture at 50°C (Fig. 4). We chose 60 minutes for glycine and L-phenylalanine, and 200 minutes for L-tryptophane. They were enough for complete breakthrough.

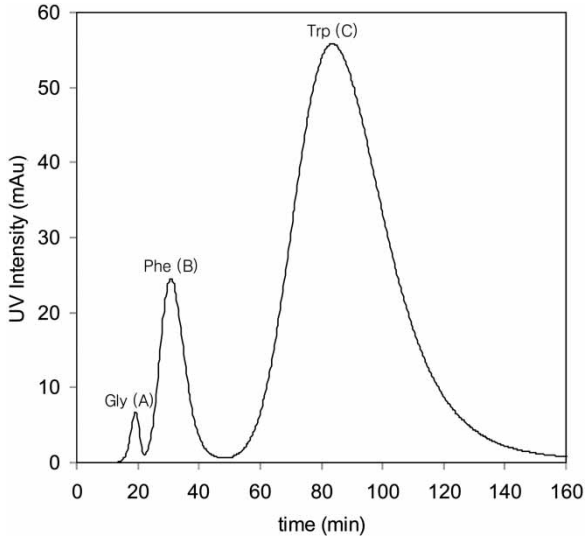

Figure 4. Concentration profiles from a pulse test of the ternary amino acid mixture at 50°C. Injection concentrations are 0.544 g/l (A), 0.970 g/l (B), and 0.408 g/l (C).

After the SMB experiments, the concentrations of the AC and B products in the two-zone SMB/chromatography system were analyzed by HPLC. The HPLC column was packed with Symmetry C18® packing (Waters Corporation, MA, US). A 20% methanol, 80% DIW mobile phase was used with a flow rate of 0.8 ml/min, and the injection volume was 3 μl. Each sample required approximately 10 minutes to analyze.

RESULTS AND DISCUSSION

Parameter Estimation

The single component isotherms were obtained from frontal tests. This analysis started from experiments without the column to obtain the dead volume. With the column present, stable plateaus were obtained for the three amino acids as shown in Fig. 5. The relation between solute concentrations in the solid q_i and liquid C_i phases shown in Fig. 6 was determined from the breakthrough times of each step in the frontal tests (41). The maximum concentrations were 0.60 g/l (A), 1.20 g/l (B), and 0.60 g/l (C). Since the three graphs show linearity with $R^2 = 96.9\%$ (A), 99.8% (B), and 99.5% (C), the linear isotherm model was used to fit the data. The results are $K_A = 0.116$, $K_B = 1.134$, and $K_C = 5.964$. Thus, the AB separation is moderate ($\alpha'_{AB} = 1.42$) and the BC separation is easy ($\alpha'_{BC} = 2.41$). The latter is the preferred condition for the two-zone SMB/chromatography system.

For mass transfer parameters, first the apparent dispersion coefficients (D_{ap}) were estimated by fitting the frontal data to the Lapidus and Amundson linear dispersion model (equation (6)). The nonlinear regression was done with Mathematica 5.0®. Then, the lumped mass transfer coefficients k_{eff} were calculated using equation (7). In this calculation, the axial dispersion D_{ax} was estimated from the Chung and Wen correlation, equation (4). The particle size ($d_p = 422.5$ μm) and $Re = 0.134$ in the frontal tests are in the range for which the correlation was derived (37). Table 2 presents the estimation results. Since five k_{eff} values were obtained from the frontal data (Fig. 5) for each amino acid, the average value was used. However, since glycine had almost no affinity to the solid phase, its mass transfer resistance was assumed to be negligible. We used $a_p k_{eff} = 1000/\text{min}$, which is large enough for very fast mass transfer in Aspen simulations. Once mass transfer is very fast, the concentration profiles become insensitive to changes in $a_p k_{eff}$. As shown in Fig. 5, the simulated and experimental profiles show good agreement. The system parameters are summarized in Table 3.

Operating Condition

Since separation at the minimum D_{total}/F will not be perfect when mass transfer resistance and axial dispersion are finite, further optimization is

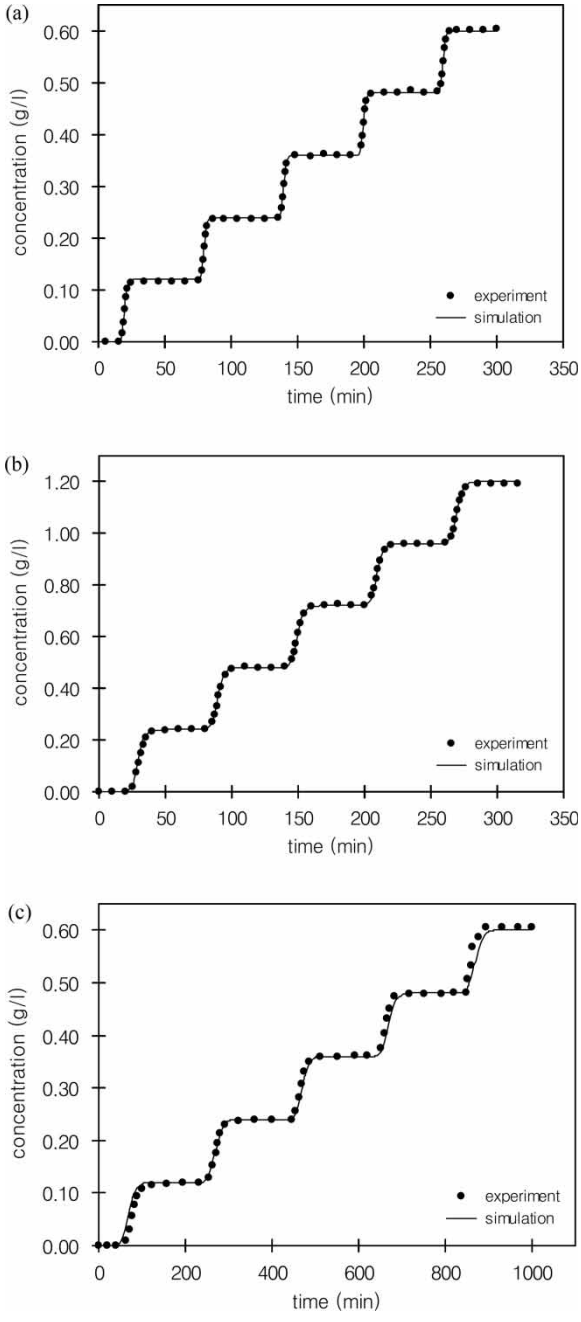

Figure 5. Concentration profiles from frontal analysis and Aspen simulation: Solid lines and circles represent simulation and experimental results, respectively. a. glycine b. L-phenylalanine c. L-tryptophane.

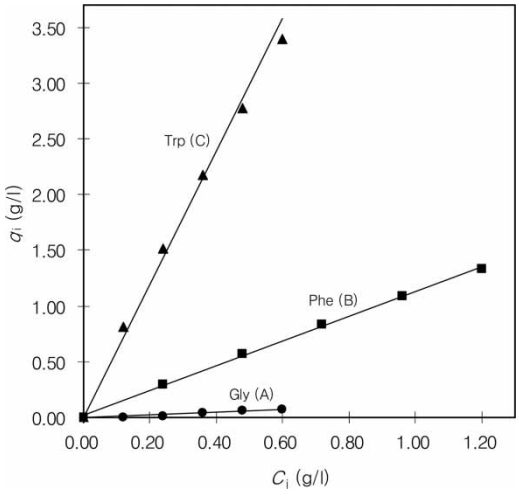

Figure 6. Isotherms from frontal analysis: Circles, squares, and triangles are calculated from frontal data of glycine, L-phenylalanine, and L-tryptophane, respectively. Solid lines are the results of linear regression.

required. Optimization tools such as the triangle theory (35), standing wave design (42), on-line optimization (43), and genetic algorithm (31, 33, 44, 45) have been developed. With the isotherms and mass transfer parameters, we used a binary coded genetic algorithm to maximize P_B. Although the genetic algorithm does not guarantee the global optimum, it has high potential because of wide-ranging search (46–49).

The objective and constraints are,

$$\text{Objective : maximize } P_B(\%)$$

$$\text{Subject to: } Q_{ij} \leq 10.0\,\text{ml/min} \tag{11}$$

$$R_B(\%) \geq 90.0\% \tag{12}$$

$$Q_{ij} \text{ and } t_j \geq 0 \tag{13}$$

The feed flow rate was 0.5 ml/min, and the maximum zone flow rate was 10 ml/min since the columns were packed at 10 ml/min. The maximum

Table 2. Axial dispersion and mass transfer parameters

Component	D_{ap} (cm^2/min)	D_{ax} (cm^2/min)[a]	$a_p k_{eff}$ (/min)
Glycine (A)	—	0.218	∞
L-phenylalanine (B)	0.427 $\pm$ 0.007	0.218	2.758 $\pm$ 0.090
L-tryptophane (C)	0.894 $\pm$ 0.067	0.218	4.204 $\pm$ 0.433

[a]Calculated from the Chung and Wen correlation (equation (4)).

Table 3. System and operating parameters

Amino Acids; Glycine (A), L-phenylalanine (B), L-tryptphane (C)	
Length of column (L), cm	30.0
Column diameter (D_{col}),cm	1.10
Total voidage (ε)	0.70
Particle diameter (d_p), μm	422.5
Fluid density (ρ), g/cm^3	0.988
Viscosity (μ), cp	0.547
Axial dispersion constant (D_{ax}), cm^2/min	Chung and Wen correlation (equation (4))
Mass transfer coefficient, 1/min	$a_p k_{effA} = 1000$, $a_p k_{effB} = 2.758$, $a_p k_{eff\ C} = 4.204$
Linear isotherm constant at T = 50°C	$K_A = 0.116$, $K_B = 1.134$, $K_C = 5.964$
Separation factor, α' (equation (2))	$\alpha'_{AB} = 1.42$, $\alpha'_{BC} = 2.41$

pressure drop is also limited by the inequality (11). For the genetic algorithm, 50 chromosomes were used, and around 4 days were required for 20 generations for which the optimum values were obtained. The time required could be reduced by using advanced techniques (44, 49). The computer program for the genetic algorithm was formulated with Visual Basic Application (VBA in Excel), and combined with Aspen Chromatography to evaluate the variables and Excel to store data. The operating condition determined from the genetic algorithm is shown in Table 4 and the total desorbent to feed ratio (D_{total}/F) was 6.24.

Simulation and Experiment

Computer simulation with Aspen Chromatography 2004® and experiments with the lab scale two-zone SMB/chromatography system (Fig. 3) were

Table 4. Operating condition for experiment

Feed concentration, g/l	Gly	0.544
	Phe	0.970
	Trp	0.408
Feed flow rate, ml/min		0.500
Desorbent flow rate, ml/min	D1	1.300
	D2	0.570
	D3	1.250
Product flow rate, ml/min	AC1	1.800
	AC2	0.570
	B	1.250
Step time, min	Step a	11.75
	Step b	11.75
Switching time, min		23.50

conducted with the operating conditions shown in Table 4. The results in Table 5 show that the simulated concentrations and purities are reasonably close to those from the experiment. The mass balance closure presents the ratio of total mass between the two products and the feed at the cyclic steady state. For Aspen simulation, numerical oscillation in the BUDS method results in the differences (40). For the SMB experiment, the low concentrations may cause inaccuracy in sample analysis. The experimental results prove that the two-zone SMB/chromatography system successfully removed 95.0% of glycine (A) and 79.2% tryptophane (C) from the ternary amino acid mixture.

Figure 7 shows the concentration history of the three amino acids in both products. While the simulated profiles of glycine and L-tryptophane match the experimental data reasonably well, L-phenylalanine shows, on average, lower concentrations in the B product than the simulations predict. This result explains why the P_B and R_B values from the experiment are smaller than the simulated values in Table 5.

Figure 8 presents the concentration profile exiting from column 2, inside of the envelope in Fig. 2. For the experimental data, samples were collected for every 2 minutes during a switching time. Since there is 1.54 ml of dead volume between the column outlet and the sampling ports, the experimental profile was adjusted using this dead volume and the flow rates of each step. The profiles of tryptophane from both simulation and experiment show considerable dispersion because of its slow mass transfer rate and long residence time in the columns. The zone spreading of tryptophane causes the low purity of the B product shown in Table 5.

Table 5. Simulation and experimental results

		AC product		B product	
		Simulation	Experiment	Simulation	Experiment
Concentration (g/l)	Gly	0.110	0.116	0.009	0.011
	Phe	0.017	0.026	0.355	0.336
	Trp	0.067	0.070	0.035	0.034
Purity (%)	Gly	56.7	54.7	2.3	2.9
	Phe	8.8	12.3	88.9	88.2
	Trp	34.5	33.0	8.8	8.9
Recovery (%)	Gly	95.8	101.1	4.1	5.0
	Phe	8.3	12.7	91.4	86.6
	Trp	77.8	81.3	21.4	20.8
Mass balance closure (%)	Gly	99.9	106.1		
	Phe	99.7	99.3		
	Trp	99.2	102.1		

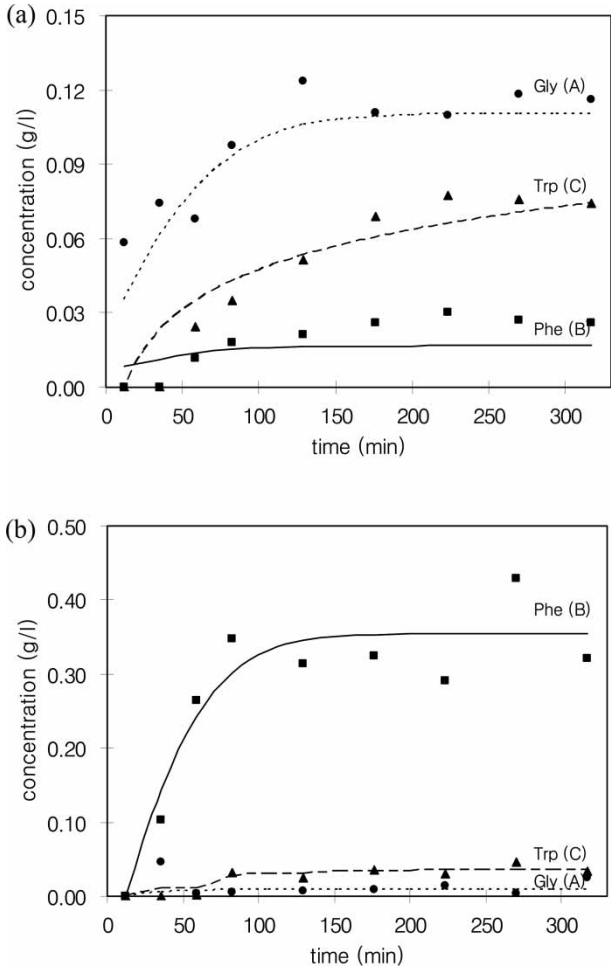

Figure 7. Concentration profiles of the product streams. Dashed, solid and long-dashed lines are the averaged concentrations obtained over a switching period from Aspen simulations. Circles, squares, and triangles show experimental data of glycine, L-phenylalanine, and L-tryptophane, respectively. a. AC product b. B product.

DISCUSSION

Compared to the standard cascade with two-four zone SMBs, since the two-zone system has a smaller number of variables, simulation and optimization are much easier and faster. In addition, the system is simple to setup and to conduct experiments. However, if the BC separation is difficult, the two-zone system may not produce a pure B product. Although our previous study showed that multiple columns per zone do not help to improve the

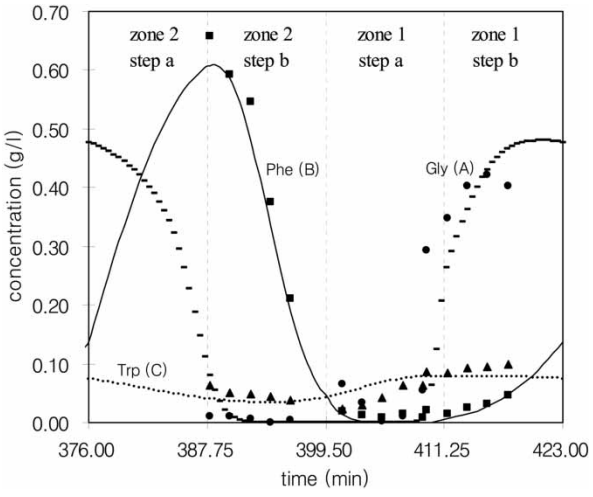

Figure 8. Concentration profiles exiting of the second column in the two-zone system (Fig. 2): Dashed, solid and dotted lines show the simulated concentration profiles and circles, squares, and triangles present experimental data of glycine, L-phenylalanine, and L-tryptophane, respectively.

two-zone system, techniques such as partial feed, selective withdrawal, and variable flow rates will probably increase the efficiency. In addition, the use of small adsorbent particles will increase mass transfer rates and should help to increase B purity by reducing both A and C fractions in the B product. The effect of the particle size can be theoretically estimated with appropriate assumptions and equations for film and pore diffusion (50).

Although we derived the D_{ax} and $a_p k_{eff}$ values in Table 2 from the apparent dispersion coefficients D_{ap} for the Aspen simulations, the D_{ap} values can be used with no mass transfer resistance $a_p k_{eff} = \infty$ since the system is linear (9). The results obtained with Aspen Chromatography simulations were close to those with separate D_{ax} and $a_p k_{eff}$ values. However, determining D_{ax} and $a_p k_{eff}$ from D_{ap} is required for reliable simulations for nonlinear systems and for scaling (50).

In Figure 6, L-tryptophane appears to be slightly nonlinear. It can be fit with the Langmuir isotherm model, $q_i = 7.128\ C_i/(1 + 0.483\ C_i)$. However, since the nonlinearity is small, the simulation results obtained with this nonlinear isotherm were similar to those with the linear isotherm in Table 3.

For the mass transfer coefficient of glycine in Aspen simulations, we simulated concentration profiles with various $a_p k_{eff}$ values ($0.1/\text{min} \leq a_p k_{eff} \leq 1000/\text{min}$) to fit the frontal data, and the results showed that the profiles are not changed for $a_p k_{eff} \geq 10/\text{min}$. Thus, we used $a_p k_{eff} = 1000/\text{min}$ for simulations, which is the default value for very fast mass transfer in Aspen Chromatography 2004®.

CONCLUSIONS

The simulation and experimental results show that the center-cut, two-zone SMB/chromatography system can be used for the separation of the intermediate retained component from ternary mixtures. With only two columns, the system removed 95.0% and 79.2% of glycine and tryptophane, respectively. Since the two-zone system is much simpler than a conventional cascade of two four-zone SMBs, it should have lower capital cost and be easier to control. However, the separation constraints are more restrictive than for the cascade with two four-zone SMBs and the B-C separation should be easy.

NOTATION

a_p	external surface area/volume, cm^2/cm^3
C	solute concentration in the liquid phase, g/cm^3
D_{ap}	apparent dispersion coefficient, cm^2/min
D_{ax}	axial dispersion coefficient, cm^2/min
D_{col}	column diameter, cm
D_{total}/F	ratio of total flow rate of desorbent to feed flow rate
erf	error function
d_p	particle diameter, cm
G_i	constant for determining the velocity of solute $= [1 + (1 - \varepsilon) K_{\text{i}}/\varepsilon]^{-1}$
K_i	linear equilibrium parameter $= q_{\text{i}}/C_{\text{i}}$
k	capacity factor $= (1 - \varepsilon) K_{\text{i}}/\varepsilon$
k_{eff}	lumped mass transfer coefficient, cm/min
L	column length, cm
P_B	purity of B in B product,%
Pe_{dp}	Peclet number based on particle diameter $= d_{\text{p}}\, v/D_{\text{ax}}$
Q	volumetric flow rate, cm^3/min
q	solute concentration on the solid phase, $g/(cm^3$ of particles)
R_{B}	recovery of B in B product,%
Re	Reynolds number $= \varepsilon\, d_{\text{p}}\, v\, \rho/\mu$
t_{sw}	switching time, min
u	solute velocity, cm/min
v	interstitial velocity, cm/min
z	axial coordinate, cm

Greek Symbols

α	selectivity based on isotherms
α'	selectivity based on solute velocities, equation (2)
ε	total bed void fraction

ρ	fluid density, g/cm^3
μ	fluid viscosity, g/(cm sec)

Subscripts

i (A, B, C)	solute, Glycine (A), L-phenylalanine (B), L-tryptophane (C)
j (1, 2)	zones in SMB
k (a, b)	step

ACKNOWLEDGEMENT

We thank Purdue University and the ERC for Advanced Bioseparation Technology, KOSEF, South Korea for partial support. Our colleagues, Weihua Jin and Ju Weon Lee offered useful suggestions in this research.

REFERENCES

1. Pynnonen, B. (1998) Simulated moving bed processing: escape from the high-cost box. *Journal of Chromatography A*, 827: 143–160.
2. Juza, M., Mazzotti, M., and Morbidelli, M. (2000) Simulated moving-bed chromatography and its application to chirotechnology. *Trends in Biotechnology*, 18: 108–118.
3. Nicoud, R.M. (2000) Simulated moving-bed chromatography for biomolecules. In *Handbook of Bioseparations*; Academic Press: San Diego.
4. Anderson, J. and Mattiasson, B. (2006) Simulated moving bed technology with a simplied approach for protein purification, Separation of lactoperoxidase and lactoferrin from whey protein concentrate. *Journal of Chromatography A*, 1107: 88–95.
5. Yu, W.F., Hidajat, K., and Ray, A.K. (2003) Application of multiobjective optimization in the design and operation of reactive SMB and its experimental verification. *Industrial & Engineering Chemistry Research*, 42: 6823–6831.
6. Antos, D. and Seidel-Morgenstern, A. (2002) Two-step solvent gradients in simulated moving bed chromatography: Numerical study for linear equilibria. *Journal of Chromatography A*, 944: 77–91.
7. Zhang, Z., Hidajat, K., Ray, A.K., and Morbidelli, M. (2002) Multiobjective optimization of SMB and varicol process for chiral separation. *AIChE Journal*, 48: 2800–2816.
8. Ludemann-Hombourger, O., Nicoud, R.M., and Bailly, M. (2000) The varicol process: A new multicolumn continuous chromatographic process. *Separation Science Technology*, 35: 2400–2411.
9. Zang, Y. and Wankat, P.C. (2002) SMB operation strategy—Partial feed. *Industrial and Engineering Chemistry Research*, 41: 2504–2511.
10. Zhang, Z., Mazzotti, M., and Morbidelli, M. (2003) PowerFeed operation of simulated moving bed units: changing flow-rates during the switching interval. *Journal of Chromatography A*, 1006: 87–99.

11. Zang, Y. and Wankat, P.C. (2002) Three-zone simulated moving bed with partial feed and selective withdrawal. *Industrial and Engineering Chemistry Research*, 41: 5283–5289.
12. Nicolaos, A., Muhr, L., Gotteland, P., Nicoud, R.M., and Bailly, M. (2001) Application of equilibrium theory to ternary moving bed configurations (four + four, five + four, eight and nine zones): I. Linear Case. *Journal of Chromatography A*, 908: 71–86.
13. Nicolaos, A., Muhr, L., Gotteland, P., Nicoud, R.M., and Bailly, M. (2001) Application of equilibrium theory to ternary moving bed configurations (4 + 4, 5 + 4, 8 and 9 zones): II. Langmuir Case. *Journal of Chromatography A*, 908: 87–109.
14. Wankat, P.C. (2001) Simulated moving bed cascades for ternary separations. *Industrial and Engineering Chemistry Research*, 40: 6185–6193.
15. Hritzko, B., Xie, Y., Wooley, R., and Wang, N.-H.L. (2002) Standing wave design of tandem SMB for linear multicomponent systems. *AIChE Journal*, 48: 2769–2787.
16. Masuda, T., Sonobe, T., Matsuda, F. and Horie, M. Process for Fractional Separation of Multi-Component Fluid Mixture. U.S. Patent 5,198,120, 1993.
17. Kurup, A.S., Hidajat, K., and Ray, A.K. (2006) Optimal operation of a pseudo-SMB process for ternary separation under non-ideal conditions. *Separation and Purification Technology*, 51: 387–403.
18. Kurup, A.S., Hidajat, K., and Ray, A.K. (2006) Comparative study of modified simulated moving bed systems at optimal conditions for the separation of ternary mixtures of xylene isomers. *Industrial and Engineering Chemistry Research*, 45: 6251–6265.
19. Beste, Y.A. and Arlt, W. (2002) Side-stream simulated moving-bed chromatography for multicomponent separation. *Chemical Engineering Technology*, 25: 956–962.
20. Kim, J.K., Zang, Y., and Wankat, P.C. (2004) Single-cascade simulated moving bed systems for the separation of ternary mixtures. *Industrial and Engineering Chemistry Research*, 42: 4849–4860.
21. Abel, S., Babler, M.U., Arpagaus, C., Mazzotti, M., and Stadler, J. (2004) Two-fraction and three fraction continuous simulated moving bed separation of nucleosides. *Journal of Chromatogaphy A*, 1043: 201–210.
22. Paredes, G., Abel, S., Babler, M.U., Mazzotti, M., Morbidelli, M., and Stadler, J. (2004) Analysis of a simulated moving bed operation for three-fraction separations (3F-SMB). *Industrial and Engineering Chemistry Research*, 43: 6157–6167.
23. Wang, X. and Ching, C.B. (2005) Chiral separation of β-blocker drug (nadolol) by five-zone simulated moving bed chromatography. *Chemical Engineering Science*, 60: 1337–1347.
24. Broughton, D.B., Neuzil, R.W., Pharis, J.M., and Brearley, C.S. (1970) The parex process for recovering paraxylene. *Chemical Engineering Progress*, 66: 70–76.
25. Kurup, A.S., Hidajat, K., and Ray, A.K. (2005) Optimal operation of an industrial-scale parex process for the recovery of p-xylene from a mixture of C_8 aromatics. *Industrial and Engineering Chemistry Research*, 44: 5703–5714.
26. Xie, Y., Mun, S., Kim, J., and Wang, N.-H.L. (2004) Standing wave design and experimental validation of a tandem simulated moving bed process for insulin purification. *Bioechnology Progress*, 18: 1332–1344.
27. Mun, S., Xie, Y., and Wang, N.-H.L. (2003) Robust pinched-wave design of a size-exclusion simulated moving-bed process for insulin purification. *Industrial and Engineering Chemistry Research*, 42: 3129–3143.

28. Wooley, R., Ma, Z., and Wang, N.-H.L. (1998) A nine-zone simulating moving bed for the recovery of glucose and xylose from biomass hydrolyzate. *Industrial and Engineering Chemistry Research*, 37: 3699–3709.
29. Kurup, A.S., Subramani, H.J., Hidajat, K., and Ray, A.K. (2005) Optimal design and operation of SMB bioreactor for sucrose inversion. *Chemical Engineering Journal*, 108: 19–33.
30. Wang, X. and Ching, C.B. (2004) Chiral separation and modeling of the three-chiral-center β-blocker drug nadolol by simulated moving bed chromatography. *Journal of Chromatography A*, 1035: 167–176.
31. Hur, J.S. and Wankat, P.C. (2006) Two-zone SMB/chromatography for center-cut separations. *Industrial and Engineering Chemistry Research*, 45: 1426–1433.
32. Hur, J.S. and Wankat, P.C. (2005) New design of simulated moving bed (SMB) for ternary separations. *Industrial and Engineering Chemistry Research*, 44: 1906–1913.
33. Hur, J.S. and Wankat, P.C. (2006) Simulated moving bed and chromatography hybrid systems for center-cut separation from quaternary mixtures: Linear isotherm systems. *Industrial and Engineering Chemistry Research*, 45: 8713–8722.
34. Ray, A.K., Carr, R.W., and Aris, R. (1994) The simulated countercurrent moving bed chromatographic reactor: a novel reactor–separator. *Chemical Engineering Science*, 49: 469–480.
35. Mazzotti, M., Storti, G., and Morbidelli, M. (1997) Optimal operation of simulated moving bed units for nonlinear chromatographic separations. *Journal of Chromatography A*, 769: 3–24.
36. Petroulas, T., Aris, R., and Carr, R.W. (1985) Analysis and performance of a countercurrent moving-bed chromatographic reactor. *Chemical Engineering Science*, 40: 2233–2240.
37. Chung, S.F. and Wen, C.Y. (1968) Longitudinal dispersion of liquid flowing through fixed and fludized beds. *AIChE Journal*, 14: 857–866.
38. Lapidus, L. and Amundson, N.R. (1952) Mathematics of adsorption in beds. VI. The effect of longitudinal dissusion in ion exchange and chromatographic columns. *Journal of Physical Chemistry*, 56: 984–988.
39. Dunnebier, G., Weirich, I., and Klatt, K.U. (1998) Computationally efficient dynamic modeling and simulation of simulated moving bed chromatographic processes with linear isotherms. *Chemical Engineering Science*, 53: 2537–2546.
40. *Aspen Chromatography: Chromatography Reference Guide*, (2001). Aspen Technology Inc.
41. Guiochon, G., Shirazi, S.G., and Katti, A.M. (1994) *Fundamentals of Preparative and Nonlinear Chromatography*; Academic Press: Boston.
42. Ma, Z. and Wang, N.-H.L. (1997) Standing wave analysis of SMB chromatography: Linear systems. *AIChE Journal*, 43: 2488–2508.
43. Abel, S., Erdem, G., Amanullah, M., Morari, M., Mazzotti, M., and Morbidelli, M. (2005) Optimizing control of simulated moving beds — Experimental implementation. *Journal of Chromatography A*, 1092: 2–16.
44. Zhang, Z., Hidajat, K., and Ray, A.K. (2002) Multiobjective optimization of simulated countercurrent moving bed chromatographic reactor (SCMCR) for MTBE synthesis. *Industrial and Engineering Chemistry Research*, 41: 3213–3232.
45. Zhang, Z., Mazzotti, M., and Morbidelli, M. (2003) Multiobjective optimization of simulated moving bed and varicol processes using a generic algorithm. *Journal of Chromatography A*, 989: 95–108.

46. Goldberg, D.E. (1989) Genetic algorithms revisited: Mathematical foundations. In *Genetic Algorithms in Search, Optimization, and Machine Learning*; Addison Wesley: Longman Inc. M.A.
47. Chambers, L. (2000) *The Practical Handbook of Genetic Algorithms Applications*; CRC Press: Boca Raton.
48. Osyczka, A. (2002) Genetic and evolutionary algorithms as a design optimization tool. In *Evolutionary Algorithms for Single and Multicriteria Design Optimization*; Physica-Verlag: New York.
49. Deb, K. (2001) *Multi-Objective Optimization using Evolutionary Algorithms*; John Wiley & Sons: New York.
50. Kim, J.K. and Wankat, P.C. (2003) Scaling and intensification procedures for simulated moving bed systems. *AIChE Journal*, 49: 2810–2821.